

Proton NMR Investigation of the Stoichiometry, Stability, and Exchange Kinetics of Tl^+ Complexes with Hexacyclen and Hexamethylhexacyclen in *N*,*N*-Dimethylformamide Solutions. Observation of a Three-Site Exchange Process

Naader Alizadeh,* Maryam Bordbar, and Mojtaba Shamsipur[1]

Department of Chemistry, School of Science, Tarbiat Modarres University, P. O. Box 14115-111, Tehran, Iran

[1]Department of Chemistry, School of Science, Razi University, Kermanshah, Iran

Received March 1, 2005; E-mail: alizaden@modares.ac.ir

^{1}H NMR spectroscopy was used to investigate the stoichiometry, stability, and exchange kinetics and mechanism of ligand interchange for Tl^+ complexes with hexacyclen (HCY) and hexamethylhexacyclen (HMHCY) in dimethylformamide (DMF) solution. In both cases, a stable complex with a 1:1 stoichiometry was formed in solution. A complete line-shape analysis was used to evaluate the mean exchange times and exchange rates. The two-site chemical exchange between Tl^+ and HCY proceeded via a dissociative ligand-interchange mechanism in the temperature range 250–310 K. However, the ^{1}H NMR spectra of the Tl^+–HMHCY complex system in DMF, in about the same temperature range, revealed the predominance of a three-site exchange process in the system. The type of exchange was dependent on the Tl^+/HMHCY mole ratio, ρ. At $\rho < 1$, ligand exchange occurs via a dissociative mechanism, while at $\rho > 1$, a bimolecular metal exchange is the predominate mechanism. In this case, the main factors controlling the exchange rates are the conformational rearrangement of the ligand during a concerted partial decomplexation of a Tl^+ cation and partial complexation of a second one. The activation parameters (E_a, $\Delta H^{\ddagger}$, $\Delta S^{\ddagger}$, and $\Delta G^{\ddagger}$) for the exchange processes (i.e. the ligand exchange, metal exchange, and the conformational change of the complex) were determined and compared with those for a two-site exchange for the Tl^+–HCY system.

The complexation behavior of polyaminomacrocycles has been extensively studied, because of their special ligational properties, which enable them to form stable complexes with both cationic and anionic species.[1–3] It has been shown that the nitrogen methylation of polyaminomacrocycles produces significant changes in the cation and anion binding features,[4,5] as well as their catalytic properties in ATP dephosphorylation in acidic media.[6] Especially, the cationic complexation of these macrocyclic ligands has been the subject of intense research work, since almost all of the transition and heavy metal ions form stable complexes with these compounds.[1–3] However, information concerning the complexation kinetics of these ligands with metal ions is rather sparse,[7,8] despite the importance of such data for the elucidating of the mechanism of complexation reactions.

A kinetic investigation of the host compounds will certainly eventually be undertaken in an attempt to better understand the specific complexation properties.[9] Two main mechanisms for the complexation of a macrocyclic ligand (L) have been proposed: The first is the so-called Chock mechanism,[10] envisaging a rapid conformational change of (L), followed by a reaction of one of the conformers of L with the cation. In this case, the rate-determining step is the complexation step, while the isomeric transformation of the ligand is relatively fast. The second is the so-called Eigen–Winkler mechanism,[11] which assumes the formation of an encounter complex, followed by a desolvation ligand rearrangement step to form the final product. In this mechanism, the rate-determining step results from a superposition of the desolvation of the metal ion and a rearrangement of the ligand. Some available data were at least qualitatively amenable for the interoperation by both mechanisms.[12]

One of the best methods to obtain insight into the solution structure of molecules is NMR spectroscopy. In the last decade, we have reported some dynamic NMR studies in several nonaqueous solvents and solvent mixtures in order to investigate the kinetics and mechanism of complexation reactions involving macrocyclic ligands and alkali, alkaline earth, and heavy metal ions.[8,13–19]

The monovalent thallium ion is a polarizable soft ion[20] with an ionic radius of 1.49 Å,[21] which has been suggested as a probe for potassium ion in biological systems.[22,23] It can substitute for K^+ ion activation of some important enzymes, such as ATP ase[24] and pyruvate kinase.[25] Thus, information about the stability and selectivity of Tl^+ complexes with macrocyclic ligands is of special interest.[2]

In the present work, we used the ^{1}H NMR method to study the stoichiometry, stability, exchange kinetics, and mechanism of Tl^+–HCY and Tl^+–HMHCY complexes in DMF solution. The special properties of HCY and HMHCY (Chart 1) were used for synthesizing thermally stable alkalides and electrides.[26–29]

Published on the web October 4, 2005; DOI 10.1246/bcsj.78.1763

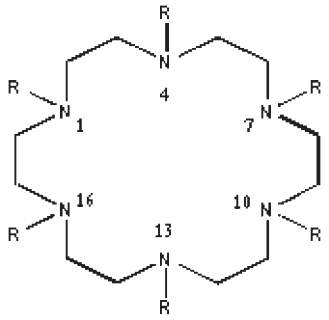

R = -H : HCY

R = -CH3 : HMHCY

Chart 1.

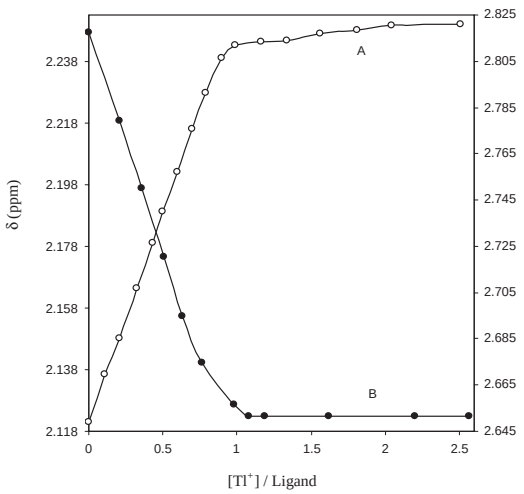

Fig. 1. Proton chemical shift as a function of Tl^+/ligand mole ratio in DMF at 300 K: (A) $-CH_2-$ protons of HCY, right scal; (B) $-CH_3$ protons of HMHCY, left scale.

Results

Stoichiometry and Stability. In order to evaluate the formation constants of the Tl^+ ion complexes with HCY and HMHCY in DMF, the proton NMR spectra of the ligands in the presence of different concentrations of Tl^+ ion were recorded at 27 °C. The resulting chemical shift vs Tl^+/ligand mole ratio (ρ) plots are given in Fig. 1. In all cases, only one average response signal was observed, indicating that the exchange rate of the cation between the bulk solution and the complexed site is fast on the NMR time scale at room temperature. As can be seen from Fig. 1, an increase in the Tl^+ ion concentration gradually shifts the corresponding proton resonance of HCY and HMHCY downfield and upfield, respectively, until a ρ value of about 1 is reached; further addition of the cation does not change the resonance frequencies considerably. This behavior is indicative of the formation of a stable 1:1 complex in both cases. The formation constants of the resulting complexes were evaluated by a computer fitting of the mole ratio data to a previously derived equation, which relates the observed chemical shift to the formation constant.[30] The resulting $\log K_f$ values were found to be >4.5 for Tl^+–HCY and >5.5 for Tl^+–HMHCY. Some increased stability of the Tl^+ complex with HMHCY over that with HCY could be most probably related to the inductive electron pumping of the $-CH_3$ groups of HMHCY, which can increase the basicity of the donating nitrogen atoms of its macrocyclic ring over that of the HCY.

Exchange Kinetics. The exchange kinetics of complexation of HMHCY and HCY with the Tl^+ ion were studied in DMF solution by ^1H NMR line-shape analysis at different temperatures. As is obvious from Fig. 1, upon complexation with the Tl^+ ion, the observed resonance frequency signals for the $-CH_2-$ protons of HCY and for the $-CH_3$ protons of HMHCY show chemical-shift changes suitable for applying the dynamic NMR technique (peak broadening was observed for $-CH_2-$ protons of HMHCY when the Tl^+ ion concentration was increased). Since the resulting 1:1 Tl^+/ligand complexes are quite stable in DMF solution, the exact population of free and complexed ligands can be directly obtained from the Tl^+ to ligand mole ratio (ρ) in a DMF solution. The proton NMR spectra of a series of solutions containing equal concentrations of the ligand, but varying concentrations of the Tl^+ ion at different temperatures, were obtained. The resulting NMR spectra are shown in Fig. 2. At the same time, and under the same experimental conditions, the NMR spectra of the free and complexed ligands were obtained, and the corresponding line widths were evaluated by fitting a Lorentzian function to the spectra. The mean lifetime of the ligand (τ) at different mole ratios and temperatures for each ligand was obtained by fitting the spectra to the appropriate NMR exchange equations (two-site exchange for Tl^+–HCY and three-site exchange for Tl^+–HMHCY system).

Tl^+–HCY, Two-Site Exchange. The ^1H NMR spectra of Tl^+–HCY in DMF at low temperatures exhibit two signals for the free and complexed ligands. Here, the mean lifetime is expressed as $1/\tau = 1/\tau_A + 1/\tau_B$, where τ_A and τ_B represent the mean residence times of the ligand on sites A (free) and B (complexed), respectively. A sample computer fit of the ^1H NMR spectra of the Tl^+–HCY system is shown in Fig. 3, and all results are collected in Table 1. In the case of the two-site exchange processes, two limiting mechanistic hypotheses exist for the exchange of a ligand between the free and complexed sites: (1) an associative–dissociative pathway and (2) a bimolecular exchange mechanism:

$$M + L \xrightarrow{k_1} ML, \tag{1a}$$

$$ML \xrightarrow{k_{-1}} M + L, \tag{1b}$$

$$^*L + ML \xrightarrow{k_{bL}} L + M^*L. \tag{2}$$

The general expression for the mean lifetime (τ) of the ligand in terms of mechanisms (1) and (2) is:[13–17,19]

$$1/\tau = k_{-1}[L]_{tot}/[L]_{free} + 2k_{bL}[L]_{tot}, \tag{3}$$

where $[L]_{tot}$ and $[L]_{free}$ are the total concentration of the ligand and the concentration of uncomplexed ligands, respectively. According to Eq. 3, at a given temperature, a plot of $1/\tau[L]_{tot}$ vs $1/[L]_{free}$ determines the contributions of these two mechanisms to the ligand interchange process. Mechanism (1) predicts the dependence of τ upon the relative population of the free ligand, while mechanism (2) predicts the dependence of τ upon the inverse total concentration of the ligand. Thus,

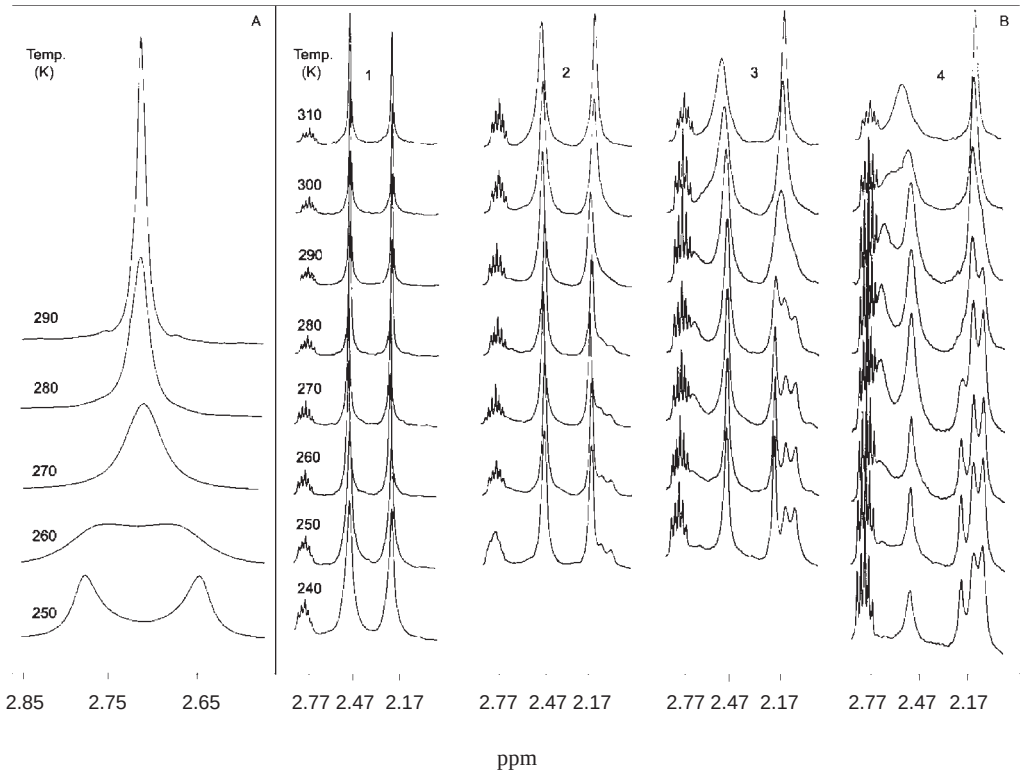

Fig. 2. Proton NMR spectra at various temperatures in DMF: (A) 0.02 M HCY with mole ratio of 0.5; (B) 0.02 M HMHCY with different mole ratios: (1) $\rho = 0$, (2) $\rho = 0.23$, (3) $\rho = 0.48$, and (4) $\rho = 0.72$.

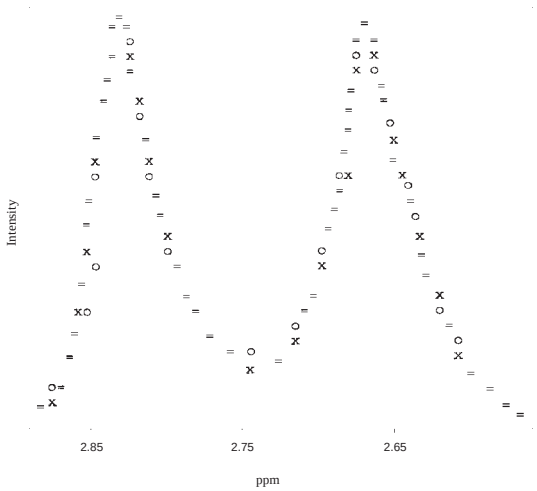

Fig. 3. Computer fit of the proton NMR spectra obtained for a Tl^+–HCY two-site exchange system with mole ratio of 0.5 at 250 K: (×) experimental point; (○) calculation point; (=) experimental and calculation points are the same within the resolution of the plot.

when the exchange process proceeds via a dissociative pathway, the $1/\tau[L]_{tot}$ vs $1/[L]_{free}$ plot results in a straight line that passes through the origin, while in the case of the predominance of a bimolecular mechanism the plot results in a line parallel to the $1/[L]_{free}$ axis. The corresponding k_{bL} and k_{-1} values for the two exchange mechanisms can then be evaluated from the intercepts and slopes of the plots of $1/\tau[L]_{tot}$ vs $1/[L]_{free}$, respectively.

Table 1. Reciprocal Mean Lifetime and Calculated Rate Constant[a)] for the Ligand Interchange of HCY Complex with Tl^+ Ion at Various Temperatures

Temp/K	$1/\tau$ (s^{-1}) Mole ratio			k_{-1}/s^{-1}
	0.21	0.53	0.80	
310	6693.4	10309.3	25062.7	5021
300	5000.0	8333.3	19493.2	3918
290	4116.9	6289.3	15479.9	2067
280	1722.1	2452.2	4972.9	886
270	711.4	1027.8	1848.4	305
260	263.2	405.5	689.7	112
250	176.7	287.4	505.1	86

a) Errors of mean lifetimes and rate constants were in the range of 2–10%.

Such plots for the Tl^+–HCY system at various temperatures are shown in Fig. 4. As is quite obvious from Fig. 4, in this system, a dissociative mechanism is predominant over the entire temperature range investigated, and the resulting exchange rate constants are also included in Table 1.

When the dissociative mechanism is dominant, a plot of $\ln k_{-1}$ vs inverse temperature gives an Arrhenius plots (see: Fig. 5). The activation energies for the release of the ligand from its Tl^+ ion complex were determined from the slopes of such plots, and the activation parameters ($\Delta H^{\ddagger}$, $\Delta S^{\ddagger}$, and $\Delta G^{\ddagger}$) were calculated by using Eyring's transition-state theory.[31] The results of these calculations are reported below.

Tl^+–HMHCY, Three-Site Exchange. The ^1H NMR spectra

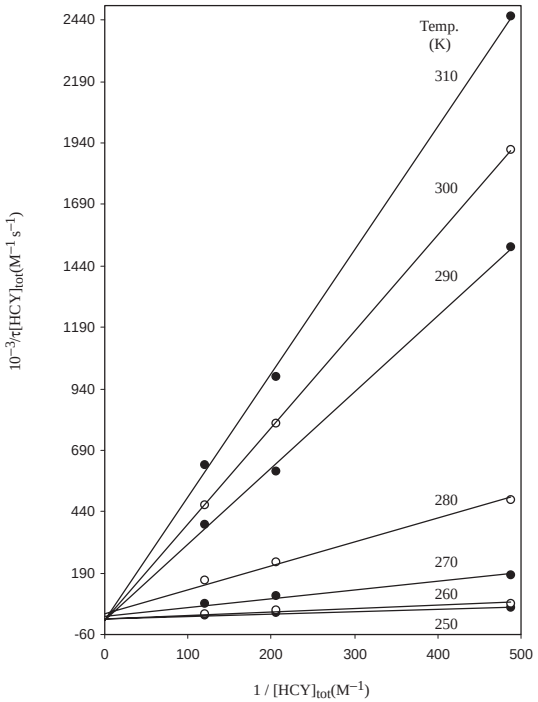

Fig. 4. Plots of $10^{-3}/\tau[HCY]_{tot}$ vs $1/[HCY]_{tot}$ for Tl^+–HCY complex in DMF at various temperatures.

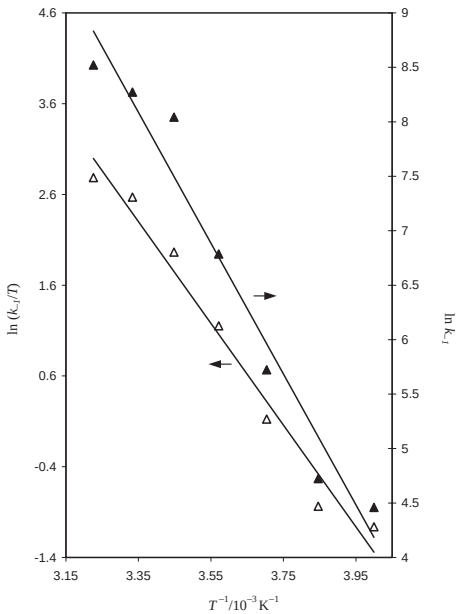

Fig. 5. Arrhenius and Eyring plots of Tl^+–HCY complex in DMF.

of the methyl protons of the Tl^+–HMHCY system in DMF solution possess a sharp line at room temperature (Fig. 2B). As the temperature of the sample is lowered, the single signal of methyl protons of HMHCY broadens and splits into three lines at $\delta = 2.245$, $\delta = 2.152$, and $\delta = 2.096$ ppm, having relative areas approximately equal to $1 - \rho$, $\rho/2$, and $\rho/2$, respectively. The area of the two peaks of equal intensity ($\rho/2$) are directly proportional to the population of the complexed HMHCY. The observation of such equal-intensity

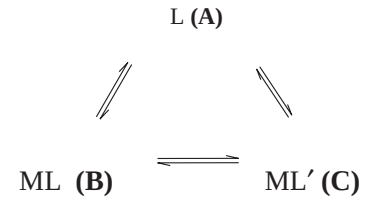

Scheme 1.

signals for the resulting thallium complex implies that, over the entire temperature range studied, in the Tl^+–HMHCY complex exists two exchangeable methyl protons (conformational forms ML and ML′ are degenerate exchange) with different magnetic environments, and since each departing methyl group is replaced by an equivalent one, it is a mutual excange, or a topomerization. As can be seen from Fig. 2B, an increase in the ρ value resulted in an increasing area of the two equivalent signals of the complexed HMHCY, while the peak intensity of the free ligand decreased. These observations in DMF solution can be reasonably explained by the three-site exchange process shown in Scheme 1.

The downfield peak in the observed spectrum, having a relative area $1 - \rho$, can be safely assigned to the free ligand (site A). However, the two upfield peaks of equal intensity are due to the two nonequivalent types of the methyl protons of HMHCY in the complexed form with Tl^+ (i.e., sites B and C). Thus, in this case, the use of a two-site equation is no longer valid to evaluate of the corresponding relaxation time values. Meanwhile, a complete line-shape analysis was conducted to determine the corresponding mean lifetimes (τ_A, τ_B, and τ_C) for the exchange processes using the modified Bloch equations for a three-site exchange mechanism.[32] Scheme 1 shows that the methyl protons have three different sites, which are labeled as A (free ligand), B (ML), and C (ML′), with the respective resonance frequencies (ν_A, ν_B, and ν_C) and populations (p_A, p_B, and p_C). The exchange routes and the labeling of the rate constants is shown in Scheme 1, and the interdependence of the corresponding populations and rate constants is given by the following equations:

$$\frac{k_{BA}}{k_{AB}} = \frac{p_A}{p_B}, \tag{4}$$

$$\frac{k_{CA}}{k_{AC}} = \frac{p_A}{p_C}, \tag{5}$$

$$\frac{k_{CB}}{k_{BC}} = \frac{p_B}{p_C}. \tag{6}$$

As is obvious, the exchange processes of this system involve a degenerate exchange with equal populations, so that Eqs. 4–6 can be simplified as:

$$\frac{k_{BA}}{k_{AB}} = \frac{k_{CA}}{k_{AC}} = \frac{p_A}{p_B}, \tag{7}$$

$$k_{BC} = k_{CB}, \tag{8}$$

$$p_B = p_C. \tag{9}$$

It can be readily shown that for the reaction path represented in Scheme 1, the observed rate laws are given by

$$-\frac{d[A]}{dt} = 2k_{AB}[A] - k_{BA}([B] + [C]), \tag{10}$$

$$-\frac{d[B]}{dt} = (k_{BC} + k_{BA})[B] - k_{BC}[C] - k_{AB}[A]. \quad (11)$$

Meanwhile, the conservation of mass implies that

$$[A] = [A]_{eq} + \Delta A, \quad (12)$$

$$[B] = [B]_{eq} + \Delta B, \quad (13)$$

$$[C] = [C]_{eq} + \Delta C, \quad (14)$$

$$-\Delta A = \Delta B + \Delta C, \quad (15)$$

where ΔA, ΔB, and ΔC are the deviations from the corresponding equilibrium values. Substitution of Eqs. 12, 13, 14, and 15 into 10 and 11, leads to

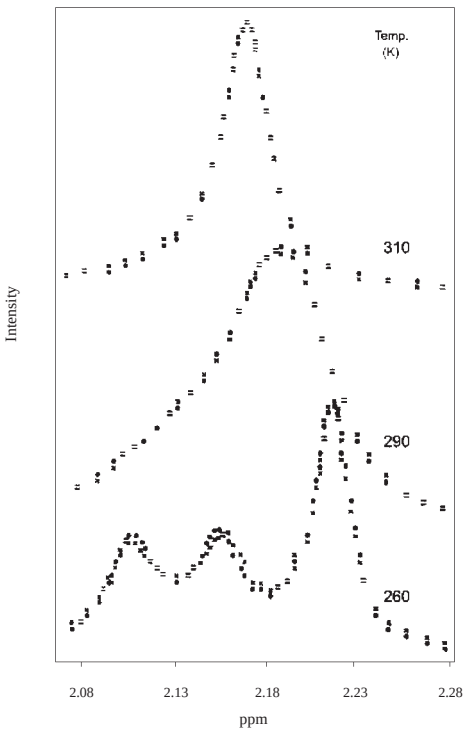

Fig. 6. Computer fit of the proton NMR spectra obtained for a Tl^+–HMHCY three-site exchange system with mole ratio of 0.5 at various temperatures: (×) experimental point; (○) calculation point; (=) experimental and calculation points are the same within the resolution of the plot.

$$-\frac{d[\Delta A]}{dt} = (2k_{AB} + k_{BA})\Delta A, \quad (16)$$

$$-\frac{d[\Delta B]}{dt} = (k_{BC} - k_{AB})\Delta A + (2k_{BC} + k_{BA})\Delta B. \quad (17)$$

The solution of Eqs. 16 and 17 results in two relaxation times (τ_1 and τ_2), given by

$$\frac{1}{\tau_1} = 2k_{AB} + k_{BA}, \quad (18)$$

$$\frac{1}{\tau_2} = 2k_{BC} + k_{BA}. \quad (19)$$

By taking into account the change in magnetization caused by jumps of the nuclei from the adjacent sites, modified Bloch equations can be obtained for an uncoupled three-site exchange of A, B, and C, the details of which are given in the Appendix. The shape function for a three-site exchange, obtained based on the corresponding modified Bloch equations, is given by Eq. 10 in the Appendix. In order to evaluate the τ_1 and τ_2 values for the three-site exchange mechanism, the line shape of the resulting ^{1}H NMR spectra (Fig. 2B) was fitted to the corresponding shape function using Powell's program.[33] Sample computer fits of the ^{1}H NMR spectra of Tl^+–HMHCY system in $\rho < 1$ at different temperatures are shown in Fig. 6, and the resulting mean lifetime (τ) values are summarized in Table 2.

Figure 7 shows the ^{1}H NMR spectra of DMF solutions of Tl^+–HMHCY at ρ values of 1, 1.5, and 3 at different temperatures. As can be seen, at a ρ value of 1, only two peaks are observed at low temperatures. As the concentration of the Tl^+ ion increases, (i.e., at $\rho = 1.5$ and 3) the exchange process becomes fast, so that only one population average signal, even at such low temperatures as 250 K, is observed. Thus, based on the previously mentioned observation, three limiting hypotheses exist for the Tl^+–HMHCY exchange system.

First, an associative–dissociative pathway occurs at $\rho < 1$, shown in Eq. 1, which consists of an associative 1a and dissociative 1b step, following the model proposed based on Eigen–Winkler mechanism.[11] The second mechanism, which also occurs at $\rho < 1$, is a bimolecular ligand interchange pathway, shown by Eq. 2. Finally, in the cases where an excess amount of the cations is present in DMF solution (i.e., at $\rho > 1$), a bimolecular metal interchange prevail. The τ expression for these three limiting cases can be obtained as follows:

Table 2. Reciprocal Mean Lifetime and Calculated Rate Constant[a)] for the Ligand and Metal Interchange of HMHCY Complexes with Tl^+ Ion at F Various Temperatures

Temp /K	$1/\tau$ (s^{-1}) Mole ratio						k_{-1} /s^{-1}	k_C /s^{-1}	k_{bL} /$M^{-1}\,s^{-1}$	k_{bM} /$M^{-1}\,s^{-1}$
	0.23	0.48	0.72	1	1.54	3.15				
310	108.9	249.7	295.9	73.0	1307.5	3141.7	—	73	—	46881
300	115.9	134.0	160.9	27.7	447.8	944.3	19	28	3607	13925
290	49.4	55.0	71.0	14.4	138.8	294.5	10	14	1415	4261
280	22.1	26.4	36.9	8.4	86.6	183.2	6	8	529	2656
270	13.4	14.9	21.9	2.8	43.3	100.0	4	3	306	1484
260	8.8	9.2	12.2	4.2	24.6	54.4	2	4	250	766

a) Errors of mean lifetimes and rate constants were in the range of 2–10%.

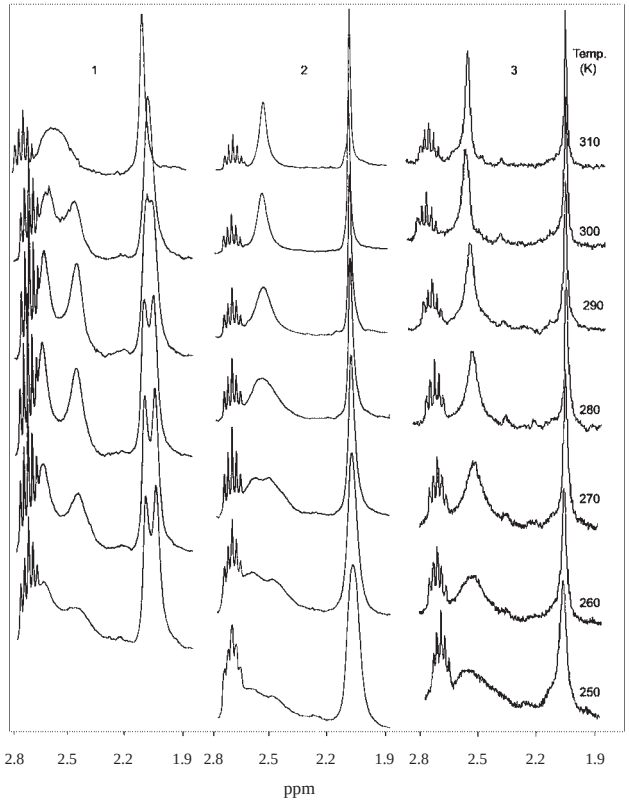

Fig. 7. Proton NMR spectra of Tl^+–HMHCY system at various temperatures in DMF with different mole ratios: (1) $\rho = 1$; (2) $\rho = 1.54$; (3) $\rho = 3.15$.

The first case is an associative–dissociative pathway:

$$1/\tau = 1/\tau_1 + 1/\tau_2, \tag{20}$$

where

$$1/\tau_1 = 2k_1[\mathrm{M}] + k_{-1}, \tag{21}$$

$$1/\tau_2 = 2k_{\mathrm{BC}} + k_{-1}. \tag{22}$$

Thus,

$$1/\tau = 2k_{-1} + 2k_{\mathrm{BC}} + k_{-1}\frac{[\mathrm{ML}]_{\mathrm{tot}}}{[\mathrm{L}]_{\mathrm{free}}} \tag{23}$$

and

$$1/\tau = k_{-1} + 2k_{\mathrm{BC}} + k_{-1}\left(1 + \frac{[\mathrm{ML}]_{\mathrm{tot}}}{[\mathrm{L}]_{\mathrm{free}}}\right) = \frac{1}{\tau_2} + k_{-1}\frac{[\mathrm{L}]_{\mathrm{tot}}}{[\mathrm{L}]_{\mathrm{free}}}. \tag{24}$$

By comparing Eqs. 20 and 24, the following final equation can be obtained:

$$1/\tau_1 = k_{-1}\frac{[\mathrm{L}]_{\mathrm{tot}}}{[\mathrm{L}]_{\mathrm{free}}}, \tag{25}$$

where $[\mathrm{L}]_{\mathrm{tot}}$ and $[\mathrm{L}]_{\mathrm{free}}$ represent the total and free concentrations of the ligand, respectively. According to Eq. 25, at a given temperature, a plot of $1/\tau_1[\mathrm{L}]_{\mathrm{tot}}$ vs $1/[\mathrm{L}]_{\mathrm{free}}$ determines the contribution of the dissociative mechanism to the exchange process.

The second case is a bimolecular ligand interchange:

$$1/\tau = k_{\mathrm{bL}}([\mathrm{ML}]_{\mathrm{tot}} + [\mathrm{L}]_{\mathrm{free}}) + 2k_1[\mathrm{M}]_{\mathrm{free}} + k_{-1}, \tag{26}$$

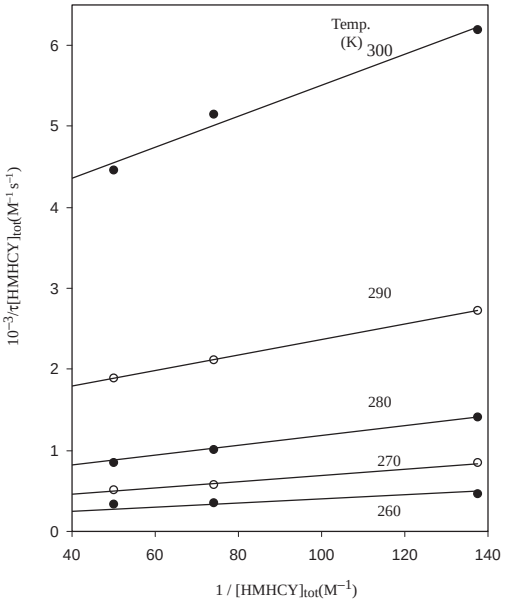

Fig. 8. Plots of $10^{-3}/\tau[\mathrm{HMHCY}]_{\mathrm{tot}}$ vs $1/[\mathrm{HMHCY}]_{\mathrm{tot}}$ for Tl^+–HMHCY complex in DMF at various temperatures.

$$1/\tau = 1/\tau_1 + k_{\mathrm{bL}}[\mathrm{L}]_{\mathrm{tot}}. \tag{27}$$

By comparing Eqs. 20 and 25, we obtain

$$1/\tau_2 = k_{\mathrm{bL}}[\mathrm{L}]_{\mathrm{tot}}. \tag{28}$$

The general expression for the τ values in terms of the two mechanisms discussed in the first and second cases (i.e., at $\rho < 1$) is as follows:

$$1/\tau = 1/\tau_1 + 1/\tau_2 = k_{\mathrm{bL}}[\mathrm{L}]_{\mathrm{tot}} + k_{-1}\frac{[\mathrm{L}]_{\mathrm{tot}}}{[\mathrm{L}]_{\mathrm{free}}}, \tag{29}$$

where k_{bL} is the bimolecular ligand interchange rate constant. According to Eq. 29, from a plot of $1/\tau[\mathrm{L}]_{\mathrm{tot}}$ vs $1/[\mathrm{L}]_{\mathrm{free}}$, the contributions from the two mechanisms can be obtained and, consequently, the rate constants, k_{bL} and k_{-1}, can be evaluated. Such plots, obtained at different temperatures, are shown in Fig. 8. The kinetic rate constants, k_{-1} and k_{bL}, were evaluated from the slope and intercept of the plot, respectively. The results are also included in Table 2.

The third case is a bimolecular metal interchange: A bimolecular mechanism for the cation interchange can be considered as follows:

$$^*\mathrm{ML} + \mathrm{M} \xrightarrow{k_{\mathrm{bM}}} \mathrm{ML} + {}^*\mathrm{M}, \tag{30}$$

and the corresponding τ value expression is given in Eq. 22 as

$$1/\tau = 2k_{\mathrm{bM}}[\mathrm{M}]_{\mathrm{free}}. \tag{31}$$

The effect of the free cation concentration on the mechanism and the rate of exchange was explored by adding different concentrations of the cation to the solution. No significant change in the chemical shift of the complex was observed in the range of $\rho = 1$ to $\rho = 3$, indicating that the corresponding concentrations of the free cation have little effect on the complexation process. However, in the presence of excess cation (i.e., at $\rho > 1$), some obvious changes in the linewidth of the NMR signal was observed, indicating the occurrence of a

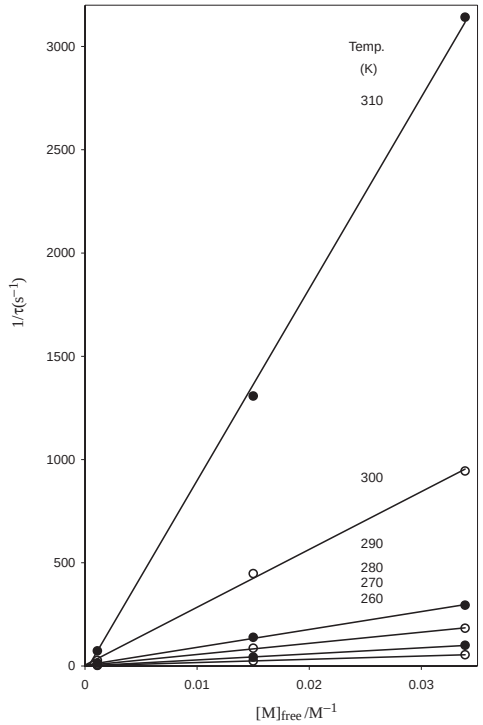

Fig. 9. Plots of $1/\tau$ vs $[M]_{free}$ for Tl^+–HMHCY complex in DMF at various temperatures.

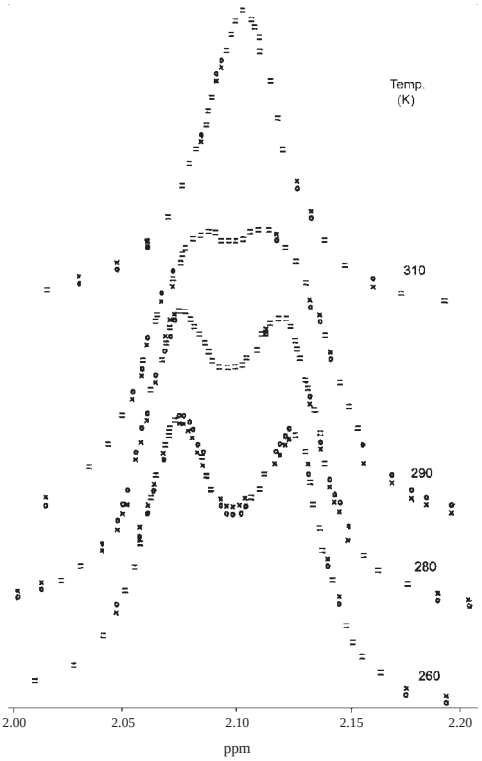

Fig. 10. Computer fit of the proton NMR spectra obtained for a Tl^+–HMHCY two-site exchange system with mole ratio of 1 at various temperatures: (×) experimental point; (○) calculation point; (=) experimental and calculation points are the same within the resolution of the plot.

metal-exchange process (see: Fig. 7). The rate constants of the metal-exchange process at different temperatures were evaluated from Eq. 31. Such plots for the metal-exchange process at various temperatures are shown in Fig. 9.

Finally, in the case of the Tl^+–HMHCY complex, the appearance of the exchange of ML with ML′ (see: Scheme 1) just begins to appear at a ρ value of 1 (Fig. 7). As is obvious from Fig. 7, at a ρ value of 1, a decrease in the temperature will result in signal broadening and its final splitting into two signals. This is a characteristic of a conformational change of the complex (from ML to ML′), the corresponding τ value of which can be written as

$$1/\tau = 2k_C. \quad (32)$$

The corresponding k_C values at different temperatures, obtained from a complete line-shape analysis using the two-site modified Bloch equations for exchange (Fig. 10) are also included in Table 2.

For all steps of the three-site exchange process, the E_a values were obtained from the Arrhenius plots of $\ln k$ values vs $1/T$ and the activation parameters ($\Delta H^{\ddagger}$, $\Delta S^{\ddagger}$, and $\Delta G^{\ddagger}$) were evaluated from Eyring's transition-state theory.[31] All of the resulting values are also included in Table 3.

Discussion

The observed changes in the pattern of the ^1H NMR spectra of the Tl^+–HMHCY system with the ρ and temperature strongly suggests the presence of two types of methyl groups in the resulting 1:1 complex. Since the ionic size of Tl^+ (about 3.0 Å) is somewhat larger than the cavity, size of HMHCY (smaller than 2.86 Å),[1] it can only partially penetrate inside the ligand cavity and will mostly remain above the plane of the ligand. A similar situation has been reported by Ellaboudy et al. for the Cs^+–HMHCY complex in the crystalline state.[29] Thus, it is not unexpected to observe different chemical shifts for the methyl protons located at the upper part of the plane of the ligand and those located in the lower part of the plane. Consequently, two types of methyl protons are observed in the ^1H NMR spectra of the Tl^+–HMHCY complex (Figs. 2B and 7). The structure of the HMHCY ring (Introduction section) has three nitrogen atoms (1, 7, and 13) in a single plane while the nitrogens (4, 10, and 16) are located below this plane. The corresponding three methyl groups attached to the planer nitrogen atoms are above the plane, and can form a rim around the basket, while the other three methyl groups are below the plane, efficiently closing the bottom of the basket. The Tl^+ ion is at the center of the cage, above the plane of the three nitrogens (1, 7, and 13) and forms a 1:1 complex. As is obvious from Figs. 2B and 7, all of the variations observed in the ^1H NMR spectra of Tl^+–HMHCY with the mole ratio and temperature clearly indicated no change in the relative population of the two types of methyl groups of HMHCY in its complex with Tl^+.

The exchange rate constants (k_{-1}, k_{bL}, k_{bM}, and k_C) were calculated, and are given in Table 2. The activation parameters for all exchange processes of the Tl^+–HCY and Tl^+–HMHCY systems in DMF were determined from the variation of the rate constants with the temperature. The resulting Arrhenius and Eyring plots are shown in Figs. 5 and 11, and the corresponding activation parameters (E_a, $\Delta H^{\ddagger}$, $\Delta S^{\ddagger}$, and $\Delta G^{\ddagger}$) are given

Table 3. Activation Parameters for the Ligand Exchange in Tl^+ Complexes with HCY and HMHCY in DMF

Ligand	Mechanism	E_a /kJ mol^{-1}	$\Delta H^{\ddagger}$ /kJ mol^{-1}	$\Delta S^{\ddagger}$ /J mol^{-1} K^{-1}	$\Delta G^{\ddagger}_{300}$ [a] /kJ mol^{-1}
HCY	Dissociative	49.9 ± 4.5 (29.3 ± 0.70)[b]	47.6 ± 4.5 (27.0 ± 0.7)[b]	-18.2 ± 1.6 (-116 ± 3)[b]	53.0 ± 0.4 (61.8 ± 0.2)[b]
HMHCY	Dissociative	38.0 ± 2.6 (31.6 ± 0.7)[b]	35.7 ± 2.6 (29.3 ± 0.7)[b]	-101.4 ± 9.4 (-97.0 ± 2)[b]	66.2 ± 0.2 (58.4 ± 0.1)[b]
	Bimolecular (Ligand exchange)	44.0 ± 7.3	41.7 ± 7.3	-40.1 ± 26.1	53.7 ± 0.6
	Bimolecular (Metal Exchange)	52.6 ± 6.3	50.2 ± 6.3	2.5 ± 22.2	49.5 ± 0.4
	Conformational Change of Complex	41.2 ± 7.1	38.8 ± 7.1	-87.0 ± 25.1	64.9 ± 0.4

a) Standard deviation calculated by using the approximate equation $\sigma(\Delta G^{\ddagger}) = |\sigma(\Delta H^{\ddagger}) - T\sigma(\Delta S^{\ddagger})|$: G. Binsch and H. Kesster, *Angew. Chem., Int. Ed. Engl.*, **19**, 411 (1981). b) The values in brackets are activation parameters in methanol.[8]

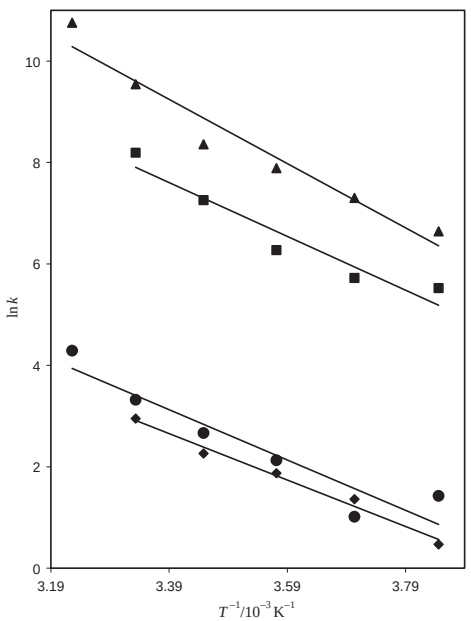

Fig. 11. Arrhenius plots of Tl^+–HMHCY complex in DMF: (▲) bimolecular metal interchange; (■) bimolecular ligand interchange; (●) conformational change; (◆) dissociative.

in Table 3. For comparison purposes, Table 3 are also includes the results previously obtained from a ^{1}H NMR study of the exchange kinetics of the Tl^+ complex with HCY and HMHCY in 70% methanol solution.[8]

In a high donating solvent, such as DMF, the solvent displacement is quite slow and the conformational change of the ligand should be the rate-determining step. For both ligands, the dissociative pathway results in negative activation entropies and positive activation enthalpies. Clearly, the exchange rates in a lower donating solvent, such as methanol, are markedly faster,[8] as compared in Table 3. It is interesting to note that the free energy required for the ligand interchange via a dissociative mechanism is nearly equal to that obtained for the interconversion process of the complex from ML to ML′.

Bimolecular processes proceed via two pathways. The first pathway proceeds via solvent displacement with the ligand, where a L′ML intermediate is generated in the presence of excess ligands ($\rho < 1$). A second pathway exists in the presence of excess metal ions ($\rho > 1$), which results in the formation of M*LM in the transition state. It should be noted that the presence of excess amounts of Tl^+ ion revealed a rather large effect on the rate of the metal interchange process.

The data given in Table 2 indicate that the rate constants of the ligand interchange are slower than those of the metal interchange, both proceeding via a bimolecular mechanism. The large positive enthalpies and entropies of activation in bimolecular mechanisms are consistent with the desolvation of the initial species and their association in the transition state. Thus, the nature of the solvent is expected to play an important role on the activation process, as shown in Table 3 (compare the results in 70% MeOH and DMF solutions).

Cox and Schneider[34] have suggested a simple mechanistic model in which the solvent molecules occupying the first coordination sphere of a metal cation are successively replaced, in a fully stepwise manner, by the donor atoms of the macrocyclic ligand. A large majority of the systems involving alkali metal cation–macrocycle complexes follow this model, as shown by NMR[35] and ultrasonic absorption techniques.[36]

Recently, the exchange kinetics of Tl^+–HCY and Tl^+–HMHCY in 70% methanol solution was studied. In both cases it was found that the exchange process occurs via a two-site exchange pathway.[8] However, in this work, the exchange process of the Tl^+–HMHCY system was found to occure via a three-site exchange mechanism in DMF solution. This means that, in Tl^+–HMHCY complex, the ligand conformational change is very fast in methanol solution, but in DMF solution, it is much slower, and consequently a significant difference in the ^{1}H NMR spectrum and the free energies of exchange were found for the Tl^+–HMHCY system (three-site exchange).

Experimental

Reagent-grade hexacyclen (1,4,7,10,13,16-hexaazacyclooctadecane, HCY) and hexamethylhexacyclen (1,4,7,10,13,16-hexamethyl-1,4,7,10,13,16-hexaazacyclooctadecane, HMHCY) from Fluka were of the highest purity available, and used as received. Analytical-grade $TlNO_3$ (Merck) was used without any further purification. Deuterated *N*,*N*-dimethylformamide (C_3D_7NO, Aldrich gold label) was used throughout. Proton NMR spectra were recorded on a Jeol JNMEX 90 FTNMR spectrometer, operating at a field

of 21.15 kG. At this field, ^{1}H resonates at 89.45 MHz. The ^{1}H NMR measurements were recorded using a 2 μs pulse width (45°), and 16 K data points were collected over a seep width of 1800 Hz. All solutions were measured in 5-mm-o.d. tubes. The temperature of the probe was adjusted with a temperature-control unit, using liquid nitrogen at low temperature and a heating element at high temperatures. To reach the equilibrium temperature, each sample tube was left in the probe for at least 10 min before measurements. At all temperatures used, the accuracy of the temperature measurement was ±0.1 °C. In all experiments, TMS was used as an internal standard. Sealed samples were used throughout. The concentration of ligands in all experiments was used 0.02 M.

Formation constants of 1:1 complexes were calculated by fitting the observed proton chemical shifts at various Tl^+/ligand mole ratios (ρ) to a previously derived equation,[30] which expresses the observed chemical shifts as a function of the free and complexed ligand and the formation constant by using a non-linear least-squares curve-fitting program KINFIT.[37] The line widths of the free and complexed ligands were measured by fitting a Lorentzian function to their spectra. A complete-line shape analysis technique was used to determine the mean lifetime (τ) for the exchange processes, using a modified Bloch equation.[38] The equations used for the two-site processes were of similar format to those used by Cahen et al.[39] Equations for the three-site exchange systems are given in Appendix. A non-linear least-squares program based on Powell's technique[33] was used to fit 50–100 points of the spectral data to the exchange equations in order to extract the τ values for each system at several temperatures.

This work has been supported by grants from the Tarbiat Modarres University Research Council, which is hereby gratefully acknowledged.

Appendix

The modified Bloch equations for an uncoupled three-site exchange of A, B, and C can be written as:

$$\frac{dG_A}{dt} = -\alpha_A G_A - iC_A + k_{BA}G_B + k_{CA}G_C - G_A(k_{AB} + k_{AC}), \tag{A1}$$

$$\frac{dG_B}{dt} = -\alpha_B G_B - iC_B + k_{AB}G_A + k_{CB}G_C - G_B(k_{BA} + k_{BC}), \tag{A2}$$

$$\frac{dG_C}{dt} = -\alpha_C G_C - iC_C + k_{AC}G_A + k_{BC}G_B - G_C(k_{CA} + k_{CB}). \tag{A3}$$

The solution of these equations for G_A, G_B, and G_C under the steady-state conditions gives the following equation for the total magnetization in the x–y plane:

$$G = G_A + G_B + G_C, \tag{A4}$$

where G is the total magnetization; G_A, G_B, and G_C are the transverse components of the contributions from sites A, B, and C to the total moment, respectively. The α_A, α_B, and α_C values in Eqs. A1–A3 are defined as follows:

$$\alpha_A = \frac{1}{T_{2A}} - 2\pi i(\nu_A - \nu), \tag{A5}$$

$$\alpha_B = \frac{1}{T_{2B}} - 2\pi i(\nu_B - \nu), \tag{A6}$$

$$\alpha_C = \frac{1}{T_{2C}} - 2\pi i(\nu_C - \nu), \tag{A7}$$

where T_{2A}, T_{2B}, and T_{2C} are the transverse or spin–spin relaxation times of A, B, and C, respectively. The separation of (4) into real and imaginary parts is considerably more lengthy than for the two-site case. After the substitution of p_AC_0 for C_A, p_BC_0 for C_B, and p_CC_0 for C_C, G takes the following form:

$$G = \frac{C_0}{\Delta}(iU - S), \tag{A8}$$

where

$$\Delta = \begin{vmatrix} -(\alpha_A + k_{AB} + k_{AC}) & k_{BA} & k_{CA} \\ k_{AB} & -(\alpha_B + k_{BA} + k_{BC}) & k_{CB} \\ k_{AC} & k_{BC} & -(\alpha_C + k_{CA} + k_{CB}) \end{vmatrix}. \tag{A9}$$

The shape function, adapted for our case of Fourier-transform spectroscopy, may be written as follows:

$$G(\nu) = C_0(I\cos\theta + R\sin\theta) + D, \tag{A10}$$

$$I = \frac{QS + UT}{Q^2 + T^2}, \tag{A11}$$

$$R = \frac{QU - ST}{Q^2 + T^2}, \tag{A12}$$

in which

$$Q = \left\{\omega_A\omega_B\omega_C - T_A(\omega_B T_C + \omega_C T_B) + \omega_A\left[\frac{1}{4}\left(\frac{1}{\tau_2} - \frac{p_A}{\tau_1}\right)^2 - T_B T_C\right] + \frac{p_A(1-p_A)}{2\tau_1^2}(\omega_A + \omega_C)\right\}, \tag{A13}$$

$$T_A = \frac{1}{T_{2A}} + \frac{1-p_A}{\tau_1};\ T_B = \frac{1}{T_{2B}} + \frac{1}{2}\left(\frac{p_A}{\tau_1} + \frac{1}{\tau_2}\right);$$
$$T_C = \frac{1}{T_{2C}} + \frac{1}{2}\left(\frac{p_A}{\tau_1} + \frac{1}{\tau_2}\right), \tag{A14}$$

$$\frac{1}{\tau_A} = \frac{(1-p_A)}{\tau_1};\ \frac{1}{\tau_B} = \frac{1}{\tau_C} = \frac{1}{2}\left(\frac{p_A}{\tau_1} + \frac{1}{\tau_2}\right);$$
$$\frac{1}{\tau_A} + \frac{1}{\tau_B} + \frac{1}{\tau_C} = \frac{1}{\tau}, \tag{A15}$$

where ω_A, ω_B, ω_C, T_{2A}, T_{2B}, and T_{2C} are the angular Larmor frequencies and the transverse relaxation times for sites A, B, and C in the absence of exchange, respectively.

$$T = -T_A(T_B T_C - \omega_B\omega_C) + \omega_A(\omega_B T_C + \omega_C T_B) + T_A\cdot\frac{1}{4}\left(\frac{1}{\tau_2} - \frac{p_A}{\tau_1}\right)^2 + (T_C + T_B)\frac{p_A(1-p_A)}{2\tau_1^2} + \frac{p_A(1-p_A)}{2\tau_1^2}\left(\frac{1}{\tau_2} - \frac{p_A}{\tau_1}\right), \tag{A16}$$

$$S = p_A S_A + p_B S_B + p_C S_C, \tag{A17}$$

$$S_A = \omega_B\left[\frac{1}{T_{2C}} + \frac{1}{2}\left(\frac{1}{\tau_1} + \frac{1}{\tau_2}\right)\right] + \omega_C\left[\frac{1}{T_{2A}} + \frac{1}{2}\left(\frac{1}{\tau_1} + \frac{1}{\tau_2}\right)\right], \tag{A18}$$

$$S_B = \omega_A\left(\frac{1}{T_{2C}} + \frac{1}{\tau_2}\right) + \omega_C\left(\frac{1}{T_{2A}} + \frac{1}{\tau_1}\right), \quad \text{(A19)}$$

$$S_C = \omega_A\left(\frac{1}{T_{2B}} + \frac{1}{\tau_2}\right) + \omega_B\left(\frac{1}{T_{2A}} + \frac{1}{\tau_1}\right), \quad \text{(A20)}$$

$$U = p_A U_A + p_B U_B + p_B U_B, \quad \text{(A21)}$$

$$U_A = \frac{1}{T_{2B}\cdot T_{2C}} + \frac{1}{2}\left(\frac{1}{T_{2B}} + \frac{1}{T_{2C}}\right)\left(\frac{1}{\tau_1} + \frac{1}{\tau_2}\right) + \frac{1}{\tau_1}\cdot\frac{1}{\tau_2} - \omega_B\omega_C, \quad \text{(A22)}$$

$$U_B = \frac{1}{T_{2A}\cdot T_{2C}} + \frac{1}{T_{2A}\cdot \tau_2} + \frac{1}{T_{2C}\cdot \tau_1} + \frac{1}{\tau_1}\cdot\frac{1}{\tau_2} - \omega_A\omega_C, \quad \text{(A23)}$$

$$U_C = \frac{1}{T_{2A}\cdot T_{2B}} + \frac{1}{T_{2A}\cdot \tau_2} + \frac{1}{T_{2B}\cdot \tau_1} + \frac{1}{\tau_1}\cdot\frac{1}{\tau_2} - \omega_A\omega_B. \quad \text{(A24)}$$

C_0, θ, and D in Eq. A10 are the amplitude, phase correction, and baseline, respectively, and τ_1 and τ_2 are the relaxation times. Eq. A10 predicts the line shape throughout the entire range of exchange from the slow limit to the fast limit for the system shown in Scheme 1.

References

1 R. M. Izatt, J. S. Bradshaw, S. A. Nielesen, J. D. Lamb, J. J. Christensen, and D. Sen, *Chem. Rev.*, **85**, 271 (1985).

2 R. M. Izatt, K. Pawlak, J. S. Bradshaw, and R. L. Bruening, *Chem. Rev.*, **91**, 1721 (1991).

3 A. Bianchi, M. Micheloni, and P. Paoletti, *Coord. Chem. Rev.*, **110**, 17 (1991).

4 A. Bencini, A. Bianchi, P. Dapporto, V. Fusi, E. Garcia-Espana, M. Micheloni, P. Paoletti, P. Paoli, A. Rodriguez, and B. Valtancoli, *Inorg. Chem.*, **32**, 2753 (1993).

5 A. Bencini, A. Bianchi, C. Giorgi, P. Paoli, B. Valtancoli, V. Fusi, E. Garcia-Espana, J. H. Llinares, and J. A. Ramirez, *Inorg. Chem.*, **35**, 1114 (1996).

6 A. Anders, J. Arago, A. Bencini, A. Bianchi, A. Domenech, V. Fusi, E. Garcia-Espana, P. Paoletti, and J. A. Ramirez, *Inorg. Chem.*, **32**, 3418 (1993).

7 R. W. Hay, R. Bembi, W. T. Moodie, and P. R. Norman, *J. Chem. Soc., Dalton Trans.*, **1982**, 2131.

8 M. Shamsipur and N. Alizadeh, *J. Chin. Chem. Soc.*, **45**, 241 (1998).

9 D. J. Cram, *Pure Appl. Chem.*, **43**, 327 (1976).

10 P. B. Chock, *Proc. Natl. Acad. Sci. U.S.A.*, **69**, 1939 (1972).

11 H. Diebler, M. Eigen, G. Ilgenfritz, G. Maass, and R. Winkler, *Pure Appl. Chem.*, **20**, 93 (1963).

12 H. Farber and S. Petrucci, *J. Phys. Chem.*, **85**, 1396 (1981).

13 M. K. Amini and M. Shamsipur, *J. Phys. Chem.*, **95**, 9601 (1991).

14 A. Rouhollahi, M. K. Amini, and M. Shamsipur, *J. Solution Chem.*, **23**, 63 (1994).

15 N. Alizadeh and M. Shamsipur, *J. Chem. Soc., Faraday Trans.*, **92**, 4391 (1996).

16 N. Alizadeh and M. Shamsipur, *J. Solution Chem.*, **25**, 1029 (1996).

17 M. Shamsipur, E. Karkhaneei, and A. Afkhami, *Polyhedron*, **17**, 3809 (1998).

18 J. Kim, M. Shamsipur, S. Z. Huang, R. H. Huang, and J. L. Dye, *J. Phys. Chem. A*, **103**, 5615 (1999).

19 M. Shamsipur, Z. Talebpur, and N. Alizadeh, *J. Solution Chem.*, **32**, 227 (2003).

20 R. G. Pearson, *J. Am. Chem. Soc.*, **85**, 3233 (1963).

21 R. D. Shannon, *Acta Crystallogr., Sect. A*, **32**, 751 (1976).

22 F. J. Kayne and J. Reuben, *J. Am. Chem. Soc.*, **92**, 220 (1970).

23 R. J. F. Williams, *Q. Rev. Chem. Soc.*, **24**, 331 (1970).

24 J. S. Britten and M. Blank, *Biochim. Biophys. Acta*, **92**, 160 (1968).

25 F. J. Kayne, *Arch. Biochem. Biophys.*, **143**, 232 (1971).

26 A. G. M. Barrett, C. R. A. Godfrey, D. M. Hollinshead, P. A. Prokopiou, D. H. R. Barton, R. B. Boar, L. Joukhadar, J. F. McGhie, and S. C. Misra, *J. Chem. Soc., Perkin Trans. 1*, **1981**, 1501.

27 G. P. Pez, I. L. Mador, J. E. Galle, R. K. Crissey, and C. E. Forbes, *J. Am. Chem. Soc.*, **107**, 4098 (1985).

28 M. E. Kuchenumeister and J. L. Dye, *J. Am. Chem. Soc.*, **111**, 935 (1989).

29 A. S. Ellaboudy, C. J. Bender, J. Kim, D. H. Shin, M. E. Kuchenmeister, G. T. Babcock, and J. L. Dye, *J. Am. Chem. Soc.*, **113**, 2347 (1991).

30 E. T. Roach, P. R Handy, and A. I. Popov, *Inorg. Nucl. Chem. Lett.*, **1973**, 359.

31 S. H. Lin, K. P. Li, and H. Eyring, "Physical Chemistry, an Advanced Treatise," ed by H. Eyring, D. Handerson, and W. Yost, Academic Press, New York (1977), Vol. II.

32 J. Sandström, "Dynamic NMR Spectroscopy," Academic Press, New York (1982).

33 M. J. D. Powell, *Comput. J.*, **7**, 155 (1964).

34 B. G. Cox and H. Schneider, *Pure Appl. Chem.*, **62**, 2259 (1990).

35 C. Detellier, H. P. Graves, and K. M. Briere, "Alkalia Metal NMR Studies of Synthetic and Natural Ionophore Complexes," in "Isotopes in the Physical and Biomedical Science; Isotopic Applications in NMR Studies," ed by E. Buncel and J. R. Jones, Elsevier Sci. Publ., Amesterdam (1991), Chap. 4.

36 E. M. Eyring, S. Petrucci, M. Xu, L. J. Rodrigguez, D. P. Cobranchi, M. Masker, and P. Firman, *Pure Appl. Chem.*, **62**, 2237 (1990).

37 V. A. Nicely and J. L. Dye, *J. Chem. Educ.*, **48**, 443 (1971).

38 J. A. Pople, W. G. Schneider, and H. J. Bernstein, "High Resolution Nuclear Magnetic Resonance," Mc Graw-Hill, New York (1959).

39 Y. M. Cahen, J. L. Dye, and A. I. Popove, *J. Phys. Chem.*, **79**, 1292 (1975).